Influence of the Central Metal Ion on Nonlinear Optical and Two-Photon Absorption Properties of Push−Pull Transition Metal Porphyrins

Paresh C. Ray,* P. Bonifassi, and J. Leszczynski

Department of Chemistry, Jackson State University, Jackson, Mississippi 39217

Received: October 1, 2007; In Final Form: December 15, 2007

We present a quantum-chemical analysis of the central metal ion's effect on first hyperpolarizabilities and two-photon absorption (TPA) cross sections at the infrared region of a series of push−pull porphyrins whose synthesis and NLO properties have been reported earlier (*J. Am. Chem. Soc.* **2005**, *127*, 9710). The molecular geometries are obtained via the B3LYP/6-31G(d,p) level optimization including SCRF/PCM approach, and the NLO and TPA properties are calculated with the ZINDO/CV method including solvent effects. It is found that the CT transition between the metal ion's d orbital and the macrocycle π orbitals plays an important role on NLO and TPA properties of metal porphyrins. Our data suggest a new approach to enhance TPA properties of porphyrin materials. We also present a quantum-chemical analysis on porphyrin dimers and trimers to understand the relationship between structural and collective NLO properties. It has been observed that β values can be improved about an order of magnitude and TPA properties can be enhanced by 2 orders of magnitude by the formation of a trimer. The importance of our results with respect to the design of photonic and photodynamic therapy materials have been discussed.

Introduction

The development of chromophores for nonlinear optics (NLO) has been driven by a multitude of important technological applications that can be realized if suitable materials are available. Future generations of optoelectronic devices for telecommunications, information storage, optical switching, and signal processing are predicted to a large degree on the development of materials with exceptional NLO responses. A large number of organic π-conjugated molecules have been investigated in the last 20 years[1−31] for suitability to function as components in hypothetical NLO materials. A few of these chromophores have served as components of functioning polymer-based optoelectronic devices; the physical properties of all these prototype materials possess one or more critical deficiencies that render commercialization of these systems impractical. These facts suggest that new types of molecular design are necessary if significant advances are to be realized. We report here a new set of engineering criteria for large molecular first-order NLO responses by varying the central metal ions in a porphyrin-based NLO chromophore structural moiety that provides significant molecular first hyperpolarizabilities by amplifying chromophore polarizability through metal-to-macrocycle charge-transfer character along the D-to-A molecular axis.

In recent years π-conjugated organic molecules with large TPA cross-section value have attracted much attention as soft processable optical nonlinear materials in light of their intensity-dependent refractive index and nonlinear absorption properties, because these features can find versatile applications in two-photon laser scanning fluorescence microscopy, optical power limiting, three-dimensional optical storage, micro-fabrication, photodynamic therapy and up-converted lasing.[32−63] These applications often rely on special organic compounds, which unite a large value of the TPA cross section at particular wavelength(s) with a specific molecular functionality. Porphyrins are unique among organic chromophores because they possess many important properties, including large excited-state absorption, long triplet lifetime, intrinsic ability of photochemical switching between tautomeric forms, as well as good biological compatibility. The study of TPA properties of porphyrins have been the focus of many recent works[35,36−40,61,62] because they are suitable candidates for the pharmaceutical industry due to their pronounced TPA in the infrared region, which can be exploited in the field of photodynamic therapy. Here we report a new set of engineering criteria for large TPA responses by varying the central metal ion in a porphyrin-based structural moiety that provides significant molecular TPA properties. Chromophore TPA properties can be amplified through metal-to-macrocycle charge transfer along the donor-to-acceptor (D-to-A) molecular axis.

In this paper, we have reported a systematic study of the NLO and TPA properties of metal porphyrins, where M = Zn, Cu, Ni, Co and Mg. We discussed the role played by metal electronic structure in determining the dimension of the NLO and TPA properties.of push−pull metal porphyrins (Scheme 1) using a combination of density functional theoretical (DFT) calculations with fairly extensive basis set [6-31G (d,p)] for geometry optimization and Zerner's Intermediate Neglect of Differential Overlap/Correction Vector (ZINDO/CV) method[20,21,26−31,63] for calculation of NLO and TPA properties. To understand how the solvent polarity affects the structure and NLO properties of the metal porphyrins, we have used self-consistent reaction field (SCRF)[64] approaches with polarizable continuum model (PCM)[65] for geometry optimization, as implemented in Gaussian 03.[66] To account for the solvent effects on TPA properties, we have adapted the ZINDO/CV technique with Onsager SCRF method.

Computational Methods

Geometry optimizations were performed at the unrestricted Kohn−Sham level utilizing the Becke3 hybrid exchange

10.1021/jp7096179 CCC: $40.75
Published on Web 02/27/2008

SCHEME 1: Structure of Push−Pull Porphyrins Used in This Manuscript

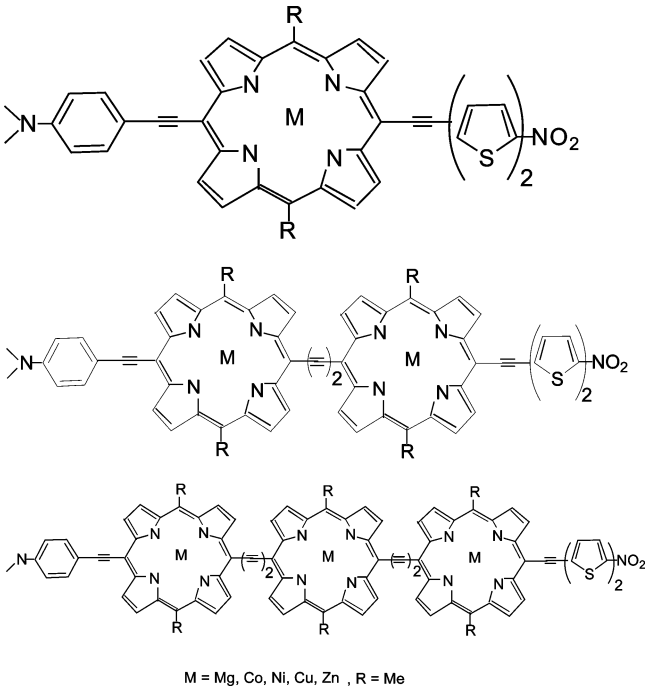

functional combined with the Lee, Yang, Parr correlation functional B3LYP as implemented in Gaussian03[66] package. The calculation has been performed with the 6-31G(d,p) basis set for carbon, hydrogen, and nitrogen. Pseudopotential LANL2DZ and its corresponding valence basis set[67] were used for the core metal. Theoretical calculations at such level has been shown to be able to reproduce experimental spectroscopic properties in a number of publications.[68,69] The optimized structure was used to calculate vibrational frequencies. Importantly, none of the frequency calculations generated negative frequencies; this is consistent with an energy minimum for the optimized geometry. We have considered the lowest spin state for each complex, chosen on the basis of experimental data, wherever available. In other complex, we have selected several multiplicities for each complex and lowest structure have chosen for NLO calculation. For the Mn complex, doublet, quartet and sextet spin states have been considered and last one termed to be the ground state. The ground states of all the other metal complexes correspond to the lower spin multiplicity are triplet for Fe, doublet for Co and Cu complex and singlet for No and Zn. To explicitly take into account the solvent polarity effects, we have adapted SCRF[64] approaches with the PCM[65] in its integral equation formalism (IEF) formulation as implemented in Gaussian 03.[66]

To calculate dynamic β values, we have adapted the ZINDO/CV technique combined with SCRF method. We have used VSTO-3G*(d,f) basis set for metals in our ZINDO calculation. The primary code for the ZINDO algorithm was developed by Zerner and co-workers,[70] and the ZINDO/SOS technique has been extensively used by several authors to compute β for different molecules.[7,36,39,57,60] Recently the ZINDO method has been combined with the correction vector (CV) technique to obtain dynamic NLO coefficients in which the sum over all the eigen states of the chosen configuration interaction (CI) Hamiltonian is exactly included.[2,20,21,26−32,46,58,63,71] We have used this technique to calculate β for the ionic and neutral weak organic acids[27] and the theoretical values match very well with the experimental data obtained via the HRS technique. The ZINDO calculation of first hyperpolarizabilities follows the CV method as described by Ramasesha et al.[26] In this method, we can obtain the NLO coefficients without resorting to the usual procedure of explicitly solving for a large number of excited states of the CI Hamiltonian, followed by a computation of the transition dipoles among these states. The first-order CV, $\phi_i^{(1)}(\omega)$, is defined by the inhomogeneous linear algebraic equation,

$$(H - E_G + \hbar\omega + i\Gamma)\phi_i^{(1)}(\omega) = \mu_i|G\rangle \tag{1}$$

where **H** is the CI Hamiltonian matrix in the chosen many-body basis, E_G is the ground-state energy, ω is the frequency, $\mu_i = \mu_i = \langle G|\mu_i|G\rangle$ is the ith component of the dipole displacement operator ($i = x, y, z$) and $\hbar/\Gamma$ is the average lifetime of the excited states. It can be shown that $\phi_i^{(1)}(\omega)$, if expressed in the basis of the eigenstates $\{|R\rangle\}$ of the CI Hamiltonian **H** is given by

$$\Phi_i^{(1)}(\omega) = \sum_R \frac{\langle R|\mu_i|G\rangle}{E_R - E_G + \hbar + i\Gamma}|R\rangle \tag{2}$$

The first-order NLO coefficients can be expressed as

$$\beta_{ijk}(\omega_1,\omega_2) = P_{ijk}\langle\phi_i^{(1)}(-\omega_1-\omega_2)|\mu_j|\phi_k^{(1)}(-\omega_1)\rangle \tag{3}$$

where the P operators generate all permutations. This method involves solving for the correction vectors in the basis of the configuration functions. The Hamiltonian matrix, dipole matrix and overlap matrix are usually constructed in the basis of configuration function, in the CI calculation. In this ZINDO/CV calculation, we have retained all singly and doubly excited configurations generated from the ground-state Slater determination by considering 20 HOMOs and 20 LUMOs. The ZINDO/CV calculation of β thus included all the excited states of the Hamiltonian in the restricted CI space. The average β values are then given by

$$\beta_{av}^i = \sum_{j=1}^{J=3} {}^1/_3(\beta_{ijj} + \beta_{jji} + \beta_{jij}) \tag{4}$$

The TPA process corresponds to the simultaneous absorption of two photons. The TPA efficiency of an organic molecule, at optical frequency $\omega/2\pi$, can be characterized by the TPA cross-sections $\delta(\omega)$. The TPA cross-section is related to the imaginary part of the second hyperpolarizability $\gamma(-\omega;\omega,\omega,-\omega)$ by[33−61]

$$\delta(\omega) = \frac{3\hbar\omega^2}{2n^2c^2}L^4\{\mathrm{Im}\}\gamma(-\omega;\omega,\omega,-\omega) \tag{5}$$

where $\hbar$ is the Planck's constant divided by 2π, n is the refractive index of medium, c is the speed of light, L is a local field factor (equal to 1 for vacuum). ZINDO/CV methodology is adopted here to calculate the second hyperpolarizabilities.

The standard expression for the (ij)th component of the transition matrix element for TPA to the state $|2A\rangle$ is given by[30,33−34,63]

$$s_{ij}(\omega) = \sum_R \left[\frac{\langle G|\mu_i|R\rangle\langle R|\mu_j|2A\rangle}{E_R - E_G - \omega} + \frac{\langle G|\mu_j|R\rangle\langle R|\mu_i|2A\rangle}{E_R - E_G - \omega}\right] \tag{6}$$

The above expression can be rewritten using the first-order CV

$$s_{ij} = \langle \phi_i^{(1)}(-\omega)|\mu_j|2A\rangle + \langle \phi_j^{(1)}(-\omega)|\mu_i|2A\rangle \quad (7)$$

Orientational average of the TPA cross-section $\delta_{TP}(\omega)$, which corresponds to the observed cross-section in solutions, is given by

$$\delta_{TP} = \frac{1}{30}\sum_{ij}(2s_{ii}s*_{jj} + 4s_{ij}s*_{ij}) \quad (8)$$

In this study, we first optimized the molecular geometries of all considered species at the DFT/PCM level in the presence of appropriate dielectric for different solvents using the Gaussian-03 package. The optimized DFT level geometry was then used as an input for ZINDO/SCRF/SOS calculation.

To compare with the experimental results, it is necessary to have a cross-section with the unit in (cm^4 s)/photon. The TPA cross-section directly comparable with experiment can be defined as

$$\delta_{max} = \frac{4\pi^3 a_0{}^5 \alpha\omega^2 g(\omega)\delta_{TP}}{c\Gamma} \quad (9)$$

where a_0 is the Bohr radius, c is the speed of light, α is the fine structure constant, and $\hbar\omega$ is the photon energy. The factor $(g(\omega)/\Gamma)$ relates the theoretical results to the shape of the exciting laser line defined by the function $g(\omega)$, and $\hbar/\Gamma$ is the lifetime broadening of the final state in atomic units. To make sensible comparison with previous results, Γ is set equal to 0.1 eV and $g(\omega)$ is assumed to be a constant, set equal to 1.

To account the solvent polarity effect in the ZINDO/CV approach, we have used expanded self-consistent reaction field (SCRF) theory[30,58,72] where self-consistent solute/solvent interactions are described by multipolar terms up to $l = 1-12$. According to this procedure the reaction field R can be defined as

$$R = g_L(\epsilon)\langle\psi|M_{lm}|\psi\rangle \quad (10)$$

where M_{lm} is the moment of the solute charge distribution and the proportional constant g is the modified Onsager factor, which can be defined as

$$g_l(\epsilon) = \frac{1}{a^{2l+1}}\frac{(l+1)(\epsilon-1)}{1+\epsilon(l+1)} \quad (11)$$

for $l = 1$ (dipolar term),

$$g(\epsilon) = \frac{2(\epsilon-1)}{(2\epsilon+1)a_0{}^3} \quad (12)$$

where ϵ is the dielectric constant of the solvent and a_0 is the radius of the spherical cavity. To find out the solvent effect in porphyrin molecules here, we have used $l = 1-12$. The cavity radius, as used in this ZINDO/CV/SCRF calculation was obtained from the Gaussian 03 code by calculating the molecular volume first, and then adding 0.5 Å to account for the nearest approach of the solvent molecules. The calculation involves the determination of molecular volume inside the cavity of electron density 0.001 electrons/$bohr^3$. We have increased the radius further by 0.5−1.5 Å and the results remains unchanged. Thus it could be assumed that the radius calculated through Gaussian is sufficient enough to encapsulate the molecule inside the cavity. To avoid resonance effect, we have used photon wavelength corresponding to 1907 nm for computing β tensors. Kanis et al. have shown[72] that ZINDO/SCRF can reproduce experimental results in donor−acceptor organic molecules reasonably well. In the above case, we first optimized the geometry at the DFT/PCM level in the presence of appropriate dielectric for different solvents using the Gaussian-03 package. The optimized DFT level geometry is then used as an input for ZINDO/SCRF/CV calculation at a photon wavelength corresponding to 1907 nm.

TABLE 1: Theoretical Dynamic First Hyperpolarizabilities (in 10^{-30} esu) for 5-[(4-(Dimethylamino)phenyl)ethynyl]-15-[5-nitro[2,2′]bithienyl-5′-ethynyl]-10,20-bis[3,5-bis((3,3-dimethylbut-1-yl)oxy)phenyl]porphinato]zinc(II), Calculated Using Different Methods and Compared with Available Experimental Values

optimization method	β calculation method	THF β	experimental[a] value
B3LYP/6-31G (d,p) /PCM	ZINDO/SOS/Onsager	782	690
B3LYP/6-31G (d,p) /PCM	ZINDO/CV/Onsager	768	

[a] Experimental value has been obtained from *J. Am. Chem. Soc.* **2005**, *127*, 9710.

To reliably estimate the TPA properties, excited-state energies, state dipoles, and transition dipole moments, we have used multireference double CI (MRDCI) formalism, where single and all higher (double, triple and quadruple) excitations have been incorporated.[30,31,46,58,71] The self-consistent field determinants, the HOMO → LUMO, HOMO → LUMO+1, HOMO−1 → LUMO, HOMO−1 → LUMO+1, HOMO−2 → LUMO, HOMO → LUMO+2, singly excited determinants and the (HOMO, HOMO) → (LUMO, LUMO) doubly excited determinants have been taken as reference determinants in the MRDCI formalism. The choice is based on the finding that these transitions dominate for one- and two-photon allowed transitions. For single excitation, the CI active space consists of 20 occupied and 20 unoccupied orbitals. For MRDCI we have used 12 occupied and 12 unoccupied molecular orbitals to construct a CI space with configuration dimension about 300 000.

Results and Discussion

The calculated M−N bond distances in CoTPP, and NiTPP are all close to 1.97 Å, notably shorter than in CuTPP, ZnTPP, and MgTPP, which are around 2.05 Å. The bond between the N and the C of the imidazole ring shows similar clustering, with the Co and Ni derivatives about 0.01 Å longer than for Cu, Zn and Mg. However, the remainder of the molecular geometry is little affected by the nature of the metal.

To calibrate our studies, we have first calculated the first hyperpolarizability of D−ZnP−A obtained by a different method and compared with experimental values (as shown in Table 1) available in the literature.[16] Comparing the magnitudes of the molecular first-order hyperpolarizabilities obtained from hyper−Rayleigh scattering (HRS) studies[16] does not require the computation of β projected onto dipole moment (μ), because the orientation averaged value is the relevant parameter and is evaluated directly. In the HRS experiment[5,10,12−19] one measures average β^2 for any molecule, where

$$\langle\beta_{HRS}{}^2\rangle = \langle\beta_{ZZZ}{}^2\rangle + \langle\beta_{XZZ}{}^2\rangle \quad (13)$$

For a dipolar molecule, $\langle\beta_{ZZZ}{}^2\rangle$ is much higher than $\langle\beta_{XZZ}{}^2\rangle$, so the main contribution arises from $\langle\beta_{ZZZ}{}^2\rangle$.[73] The relation between $\langle\beta_{ZZZ}{}^2\rangle$ in laboratory coordinates and $\langle\beta_{zzz}{}^2\rangle$ in the molecular

reference frame has been discussed in detail by Bershon et al.[74] and Clays et al.[73] and the relation can be expressed as

$$\langle\beta_{ZZZ}{}^2\rangle = {}^1/_7\sum_i\beta_{iii}{}^2 + {}^6/_{35}\sum_{i=j}\beta_{iii}\beta_{ijj} + {}^9/_{35}\sum_{i=j}\beta_{iij}{}^2 + {}^6/_{35}\sum_{ijk,\mathrm{cycl}}\beta_{iij}\beta_{jkk} + {}^{12}/_{35}\beta_{ijk}{}^2 \quad (14)$$

Here, cyc means cyclic permutation of co-ordinate indexes. In HRS expression, an isotropic average is made for the molecule's all β tensor components, indicating that the HRS is sensitive to all such elements. For dipolar molecules, where the molecular tensor components in the direction of the charge-transfer axis is the largest, the values of $\langle\beta_{ZZZ}\rangle$ and $\langle\beta_{zzz}\rangle$ are expected to be the same. We have calculated β_{zzz} and β_{ZZZ} (using eq 14) for D−ZnP−A compound. Our results indicate that β_{zzz} and β_{ZZZ} values are comparable and within 3−5% error. So, though in a typical HRS experiment one detects the sum of two polarizations, an error of only 5−10% will be introduced if the other tensor components are neglected for the push−pull chromophores we are dealing with in this manuscript. So it is appropriate to compare the β_{HRS} with our calculated $\beta_{ZINDO/CV}$. Table 1 shows that our calculated ZINDO/CV β values are in 15% agreement with the experimental value. As a result we have used ZINDO/CV method to calculate the first hyperpolarizability of other metal porphyrins.

Calculations have been done assuming a uniform empirical broadening parameter $\Gamma = 0.1$ eV and $\Gamma = 0.12$ eV for dimers and $\Gamma = 0.15$ eV for timers which is not the case for real molecular systems. The point to be noted is the fact that the theoretical calculations focus on the maximum limit of the resonant two-photon absorption cross-section, which is an intrinsic property of the molecule. When the molecule is placed in a material made of a collection of molecules, the resonance peak gets smaller and broadened. Ahn et al.[41] and Drobizhev et al.[42] have measured the lifetime for porphyrin and its covalently linked dimer, trimer and tetramer. Their results show that lifetime decreases from monomer to covalent aggregates and so Γ should increase with aggregation. For homogeneous broadening to be taken into account, the natural line-widths need to be known for our system, and this is seldom the case. To simulate the experimental inhomogeneously broadened absorption profile, one needs to perform summation of the absorption amplitudes over vibrational levels of the first excited electronic state. Unfortunately, for a system with hundreds of vibrational modes the problem of evaluating the generalized Franck−Condon amplitude is not a trivial one. Because we do not have actual experimental values, to make a sensible comparison, we have used $\Gamma = 0.1$ eV monomer and $\Gamma = 0.12$ eV for dimers and $\Gamma = 0.12$ eV for timers.

ZINDO/CV methodology is adopted here to calculate the second hyperpolarizabilities. Recently, several publications[16,25,31,46,57−59] have shown that the ZINDO/CV or ZINDO/SOS model allows obtaining first hyperpolarizabilities and TPA properties of porphyrin monomer and dimer that can be directly compared with the outcome of the experimental measurements. To calibrate our studies, we have first calculated (as shown in Table 2) the TPA cross-section of *meso*-butadiyne-linked symmetrical porphyrin monomer and dimer whose experimental values are known. We note that our calculated ZINDO/CV δ values are in 80% agreement with the experimental value and the increment pattern follows nicely as we move from monomer to dimer.

Table 3 shows how β values change with the central metal ions for porphyrin dimers. We have also calculated β values for same donor−acceptor (D−A) porphyrins dimers without any central metal. Our calculation shows $\beta = 98 \times 10^{-30}$ esu for nonmetal D−A porphyrins. It is interesting to note that metalloporphyrins with strong CT transitions in their one-photon absorption spectra have β values that are an order of magnitude larger than that of the porphyrin with nonmetal. Even within the transition metal porphyrins, variation of metal ions can enhance the first hyperpolarizability, β, by at least half an order of magnitude. Therefore, a well-designed metal D−A prophyrin (DAP) system could be an excellent candidate for application in second harmonic generation as well as for electrooptic devices based on Pockels effect.

TABLE 2: Theoretical Two-Photon Absorption Cross-Section (in 10^{-50} (cm^4 s)/photon) for *meso*-Butadiyne-Linked Symmetrical Porphyrin, Calculated Using ZINDO Methods and Comparison with Available Experimental Values

$\langle\delta_{max}\rangle$ calculation method	$\langle\delta_{max}\rangle$ monomer	$\langle\delta_{max}\rangle$ dimer
ZINDO/SOS/Onsager	24	4200
ZINDO/CV/Onsager	26	4800
experimental[a]	20	5500

[a] Experimental values have been obtained from *J. Phys. Chem. B.* **2005**, *109*, 7223.

TABLE 3: Theoretical (ZINDO/CV/SCRF) One-Photon Q-Band Absorption Wavelength (λ_{max} in nm), Oscillator Strength and Dynamic First Hyperpolarizabilities (in 10^{-30} esu) and Dipole Moment Change Between Ground and Excited States ($\Delta\mu$ in Debye) for Porphyrins with Different Central Metal Ions

metal	λ^{max}	f	β	$\langle\Delta\mu\rangle$
Mg	768	1.74	3600	41.2
Co	709	.150	930	23.4
Ni	725	.690	1480	25.8
Cu	746	1.36	2070	29.3
Zn	762	1.61	2340	31.6

To understand the origin of the change in hyperpolarizabilities due to the variation of central metal ions, we have calculated λ_{max} and the change in dipole moment between ground and charge-transfer excited state ($\Delta\mu_{eg}$). According to the two-state model,[75−77]

$$\beta^{\text{two state}} = \underbrace{\frac{3\mu_{eg}{}^2\,\Delta\mu_{eg}}{E_{eg}{}^2}}_{\text{static factor}}\ \underbrace{\frac{\omega_{eg}{}^2}{(1-4\omega^2/\omega_{eg}{}^2)(\omega_{eg}{}^2-\omega^2)}}_{\text{dispersion factor}} \quad (15)$$

where μ_{eg} is the transition dipole moment between the ground state $|g\rangle$ and the charge-transfer excited state $|e\rangle$, $\Delta\mu_{eg}$ is the difference in dipole moment and E_{10} is the transition energy. The first excited state of all the compounds under investigation is strongly associated with the HOMO−LUMO transition. A detailed analysis of these orbital characters should provide a better understanding for the behavior of the systems. λ_{max}, oscillator strength (f) and $\Delta\mu_{eg}$ vales are also listed in Table 3. For metal ion donor−acceptor porphyrins (DAP), mixing of the metal d and macrocycle π orbitals leads to additional peaks in the absorption spectrum. For D−MP−A, these CT transitions involve the $\pi(a_{1u},a_{2u})$ orbitals of the macrocycle and the metal ion's d_π orbitals ($\pi \rightarrow d_\pi$). These CT transitions are allowed as they occur between electronic states of opposite symmetry (g $\rightarrow$ u). Our calculation shows that Q-band f value is quite high for Mg, Cu and Zn, moderate for Ni and quite low for Co. The absence of strong CT bands in the Co DAP suggests that the mixing of the Co ion's d orbitals with the macrocycle's π system is less efficient and as a result β is low. Thus, comparison of nonlinear optical properties of Co TPP and Mg, Cu or Zn DAP

TABLE 4: Theoretical (ZINDO/CV/SCRF) Single Photon Q-band Absorption (λ^{SPA} in nm), Oscillator Strength, Two-Photon Absorption Wavelength (λ^{TPA} in nm) and Two-photon Absorption Cross-sections (δ_{max} in 10^{-50} (cm^4 s)/photon) and Dipole Moment Change Between Ground and Excited States ($\Delta\mu$ in Debye) for Porphyrins for Porphyrins with Different Central Metal Ions

metal	λ^{SPA}	f	λ^{TPA}	$\langle\delta_{max}\rangle$	$\langle\Delta\mu\rangle$
Zn	701	1.52	1380	8500	26.5
Mg	717	1.54	1460	21200	35.6
Cu	695	1.26	1310	7600	24.8
Ni	678	.680	1240	6800	20.6
Co	663	.180	1180	2200	18.7

allows understanding the role of metal ion/macrocycle interactions on first hyperpolarizabilities of donor−acceptor metal porphyrins.

Our calculations indicate that the increment of first hyperpolarizability in Mg, Cu or Zn DAP compared to Co DAP is due to two factors, and these are (1) the red shift and higher oscillator strength of the CT band, which brings it closer to the peak of the two-photon resonance wavelength, and (2) $\Delta\mu_{eg}$ values varying about 1.4−1.9 times with the change of metal substituents. As we noted in Table 3, $\Delta\mu_{eg}$ vales follow the same trend with β for D−A porphyrins with different metal substituents. This confirms that $\Delta\mu_{eg}$ could be one of the main factors for the effect of metal substitution on the first hyperpolarizabilities of metal porphyrins.

Table 4 shows how central metal ions affects δ_{max} values. We have also calculated δ_{max} values for same donor−acceptor (D−A) porphyrins without any central metal. Our calculation shows $\delta_{max} = 220 \times 10^{-30}$ esu for nonmetal D−A porphyrins. It is interesting to note that metalloporphyrins with strong CT transitions in their one-photon absorption spectra have δ_{max} values that are more than an order of magnitude larger than that of the porphyrin with nonmetal. Our results explain the recent experimental report by Humphrey et al.,[11] that metalloporphyrins with strong CT transitions in their one-photon absorption spectra have δ values that are an order of magnitude larger than those of the free base porphyrin. Our calculations indicate that even within the transition metal porphyrins, variation of metal ions can enhance the δ_{max} at least by an order of magnitude. Therefore, a well-designed metal D−A prophyrin (DAP) system could be an excellent candidate for application in three-dimensional optical storage, micro-fabrication and photodynamic therapy.

The electronic spectra of porphyrin derivatives are usually interpreted using the four orbital model of Gouterman,[77] which assumes that the HOMO (a_{2u}/a_{1u}) and HOMO−1 (a_{1u}/a_{2u}) of a porphyrin molecule are nearly degenerate, and the LUMO and LUMO−1 (e_g*) are rigorously degenerate. The first excited state is a strong CT state, possessing intense one-photon absorption cross sections.

Our results indicate that in our donor−metal porphyrin−acceptor (D−MP−A) compounds, mixing of the highest occupied orbitals of the metal porphyrin (MP) bridge with the donor (D) fragment leads to a nearly degenerate HOMO. It is also worthy to note that the LUMO+1 and LUMO+2 in D−MP−A become degenerate due largely to the strong mixing of the porphyrin-based π-orbital with those of the acceptor (A) fragment. Thus, in our D−MP−A compounds, the frontier orbitals have significant contributions from the π-orbitals of the D and A fragments. It is noticed that the HOMO and the LUMO both show very strong charge separation but with opposite sign. In the HOMO, the charge is mainly located on the electron donor side, whereas in the LUMO, it is gathered on the electron acceptor side. The energies of these porphyrin MOs are sensitive to the nature of the particular metal (as shown in Figure 1). As one moves across the periodic table from Mg to Zn, the energies of the metal d-orbitals tend to drop. This pattern is most evident and dramatic in the $d_{x^2-y^2}$ orbital. The difference in energy between the HOMO and LUMO of each of the various TPP complexes is reported in Table 4. As one goes across the periodic table from Mg to Zn, there is a fluctuating trend in these energy gaps. The gap increases from Mg to Co, then decreases through Ni and Cu, before rising again in the case of Zn. One- and two-photon $\lambda_{max,}$ oscillator strength (f), δ_{max} and $\Delta\mu_{eg}$ vales are also listed in Table 4. For metal ion donor−acceptor porphyrins (DAP), mixing of the metal d and macrocycle π orbitals leads to additional peaks in the absorption spectrum. For D−MP−A, these CT transitions involve the π-(a_{1u},a_{2u}) orbitals of the macrocycle and the metal ion's d_π orbitals ($\pi \rightarrow d_\pi$). These CT transitions are allowed as they occur between electronic states of opposite symmetry. Our calculation shows that Q-band f value is quite high for Mg, Cu and Zn, moderate for Ni and quite low for Co. The absence of strong CT bands in the Co DAP suggests that the mixing of the Co ion's d orbitals with the macrocycle's π system is less efficient and as a result δ_{max} is low. Thus, comparison of Co TPP and Mg, Cu or Zn DAP nonlinear optical properties allows understanding the role of metal ion/macrocycle interactions on TPA properties of donor−acceptor metal porphyrins. The increase in conjugation length and the enhancement of the strengths of the electron donor/acceptor change the appearance of the orbitals. The charge separation becomes even more profound. But the basic characters of these two orbitals are kept the same as those for the DP−ZnP−DA compound.

To understand the origin of high TPA properties of D−A porphyrins, we have used two-level model where the TPA cross-section can be defined as[49−53,58]

$$\delta_{2-state} = \frac{4\pi^2 a_0^5 \alpha\omega^2}{15c_0} \frac{M_{ge}^2 \Delta\mu_{ge}^2}{E_{ge}^2 \Gamma} \qquad (16)$$

where a_0 is the Bohr radius, c_0 is the speed of the light, α is the fine structure constant, ω is the photon energy, M_{ge} is the transition dipoles between the ground state $|g\rangle$ and a TPA state $|e\rangle$. $\Delta\mu_{ge}^2$ denotes the square of the change in dipole moment between ground and excited charge-transfer (CT) states, and E_{ge} is the transition energy between the ground state $|g\rangle$ and a TPA state $|e\rangle$. $\Delta\mu_{ge}$ values for all the D−A monomer porphyrins are also reported in Table 4. The trend is for variation of TPA properties, but $\Delta\mu$ and M_{ge} are same with the variation of central metal ions (as shown in Figure 2). The results of our calculation indicate that, as the charge-transfer character of the ground electronic state increases with increasing donor strength, (i) a drastic increase of change in dipole moment between ground and excited CT states occurs, (ii) the transition dipole matrix elements $|M_{eg}|$ amplitude increases monotonically, and (iii) E_{ge} decreases monotonically.

To understand how the first hyperpolarizabilities and TPA properties are influenced by aggregation, we have studied the NLO and TPA properties of dimer and trimer of D−A porphyrins, where porphyrin monomers are connected with each other through two carbon−carbon triple bonds. The insertion of the two carbon−carbon triple bonds between two porphyrin rings has effects on the geometrical and electronic structures of the molecules. The D−MP−(≡)$_2$ −MP−A compound is highly planar compared to D−MP−[≡]−MP−A. Such conjugated planar structure can increase the conjugation length of

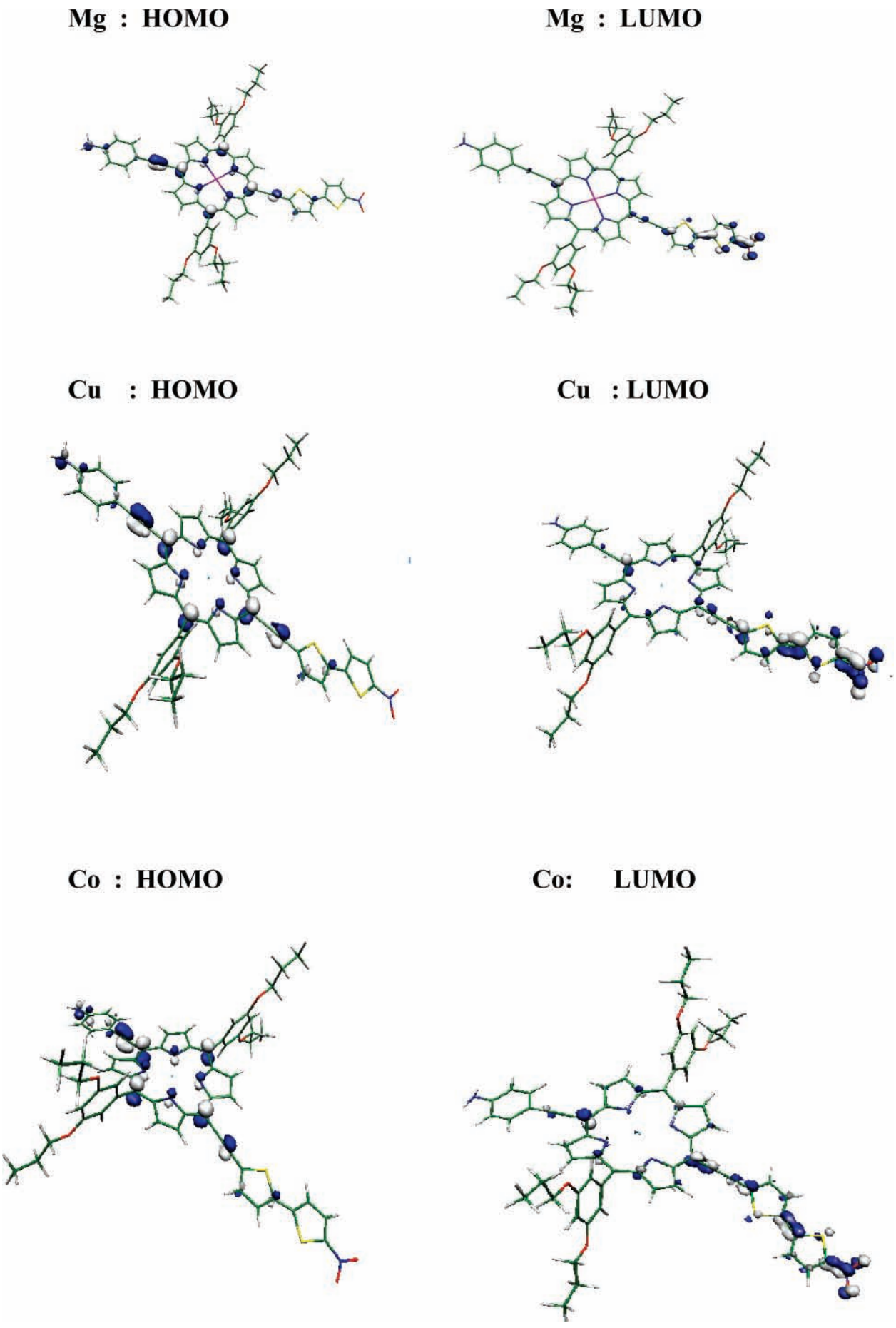

Figure 1. Part 1 of 2.

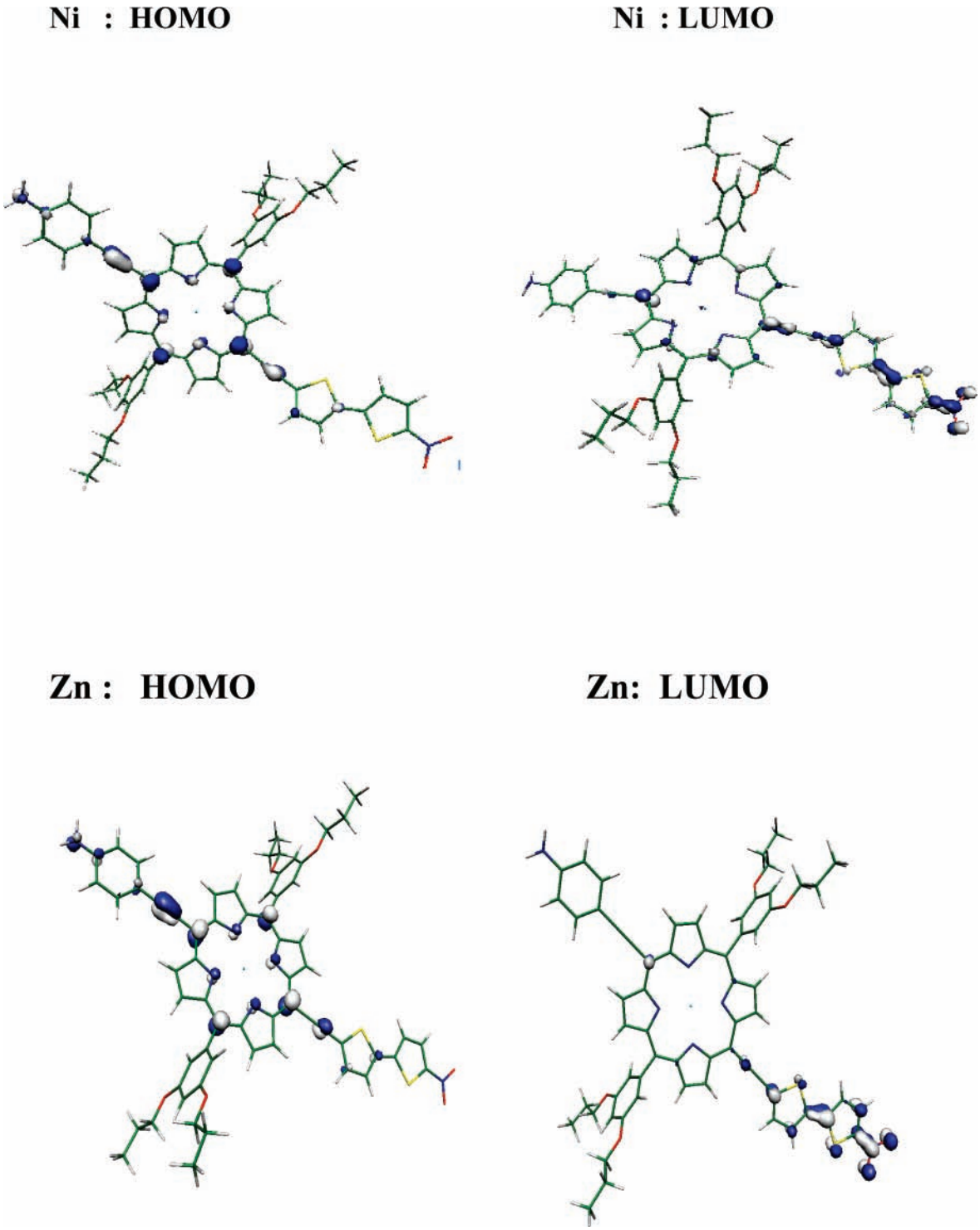

Figure 1. Part 2 of 2. Electron distributions of the LUMO and the HOMO of D−M−A porphyrins with M = Mg, Cu, CO, Ni and Zn.

the π electron and make the system more polarizable. Comparing the single photon absorption, all metal porphyrin dimers show some common spectroscopic trends, when compared with the monomer. First, the lowest energy Q-band is drastically intensified and red-shifted, and second, the Soret (B) band splits over several sub-bands, whose center also shifts to the red. It is noteworthy that the considerable amplification of the Q-band in dimer is one of the key factors governing the enhancement of β values and TPA response in the near-IR. Our calculations indicate that due to a strong electronic interaction (molecular orbital overlapping) between two porphyrin rings in dimer, the four Gouterman frontier orbitals of the monomer split into at least eight frontier orbitals which qualitatively describes the complexity of the spectrum and explains the significant intensification of the lowest $S_0 \rightarrow S_1$ (Q) transition. Another possible reason for the intensification of the Q-transition is an extension of conjugation length simply because of dimerization. Figure 3 shows how β values are influenced by the central metal ions for dimers and trimers. We also added monomer values for comparison. It is interesting to note that within the transition metal porphyrins, variation of metal ions can enhance the β values by at least half an order of magnitude and the effect of central metals ions is similar for all cases, monomer, dimer and trimer. Our calculations indicate that as the β value increases

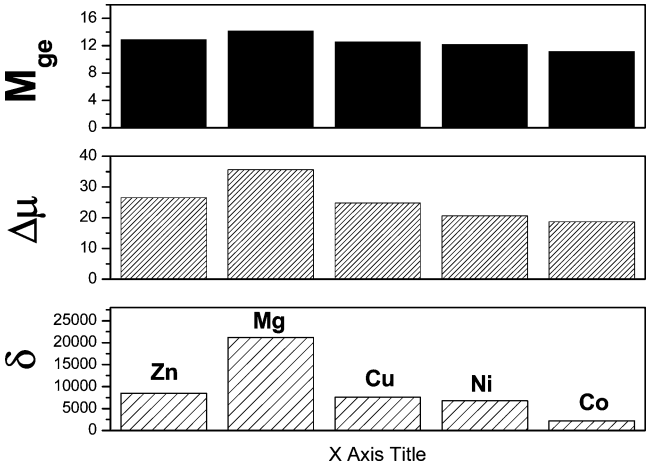

Figure 2. Variation of δ_{max}, $\Delta\mu$ and M_{ge} with change of metal substituent for monomer.

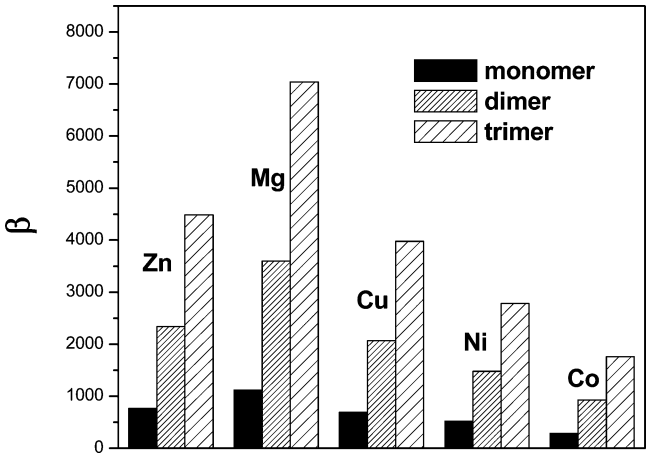

Figure 3. Influence of metal ions on β vales of D−A porphyrin for monomer, dimer and trimer.

three times as we move from monomer to dimer and two times as we more from dimer to trimer. Our calculation results can explain recent experimental reports on extremely high β values in conjugated porphyrin dimers.[12,18,19] Our calculation indicates that, by increasing the number of monomers, (i) change in dipole moment between ground and excited charge-transfer (CT) states increases, (ii) the transition dipole matrix elements $|M_{eg}|$ amplitude increases, and (iii) E_{ge} decreases, as a result β values increases tremendously. So we have shown that by choosing a proper central metal ion with porphyrin timers, one can enhance the NLO properties by about 30 times with respect to the well studied Zn porphyrin monomer. Such amplification of chromophore polarizability through the engineering of metal-to-macrocycle charge-transfer character along the D-to-A molecular axis suggest a very good approach to enhance optical properties of porphyrin materials and new design direction for NLO compounds which can have several advantages.

The two-photon absorption maxima shows high red shift toward desirable wavelengths of (800−2000) nm as we move from monomer to dimer to trimer. The calculated λ^{TPA} is observed 1460 nm for Mg porphyrin monomer, 1780 nm for dimer and 1960 nm for trimer. A similar red shift in maximum TPA wavelength is observed for other metal porphyrins.

As shown in Figure 4, the maximum TPA cross-section increases about an order of magnitude from monomer to dimer and about 6−8 times as we move from dimer to trimer. Our calculation results can explain recent several experimental reports on extremely strong near-IR two-photon absorption of

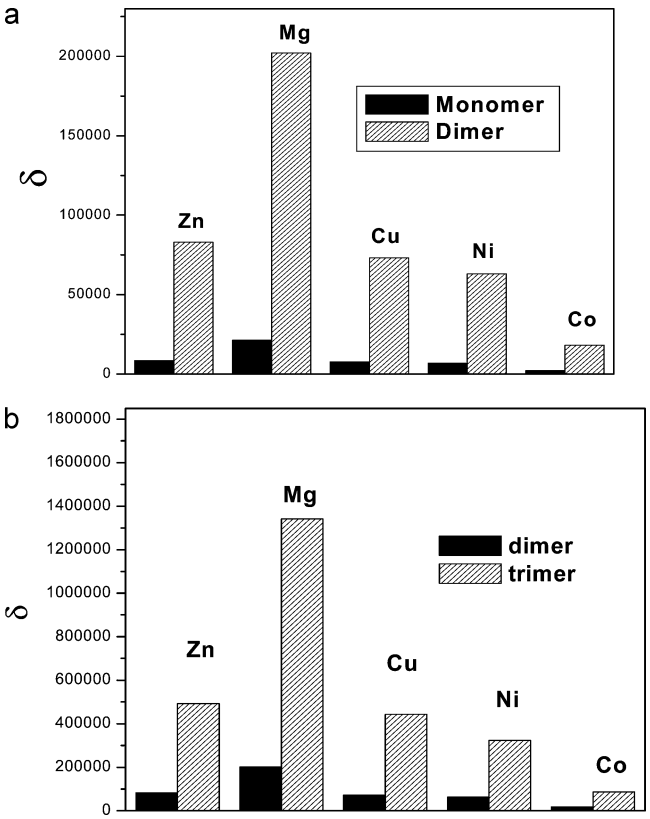

Figure 4. δ_{max} of metal D−A porphyrins for (a) monomer, dimer and (b) dimer and trimer.

conjugated porphyrin dimers.[33,34,41,42] Our results suggest that maximum TPA cross section can be enhanced 2 orders of magnitude for the trimer when compared to monomer (as shown in Figure 4). Therefore, a well-designed D−A prophyrin trimer system could be an excellent candidate for application in biological imaging and photodynamic therapy. In fact, the largest TPA cross-section obtained, 2.12×10^6 GM (Goppert-Mayer units), is the largest TPA cross-section values reported in the literature for organic or organometalic compounds. For all dimer and trimer chromophores under investigation, the first excited state is a CT state, possessing both strong one- and two-photon absorption. According to the two-state model, the transition dipole moment to the CT state and dipole moment changes between ground and CT states are the two key parameters controlling the magnitude of the TPA cross section. Our calculation shows that the trend of the variation of TPA properties, M_{ge} and $\Delta\mu$ are similar. We have noted the same trend for trimer.

Conclusion

In this manuscript we have explored the role played by metal electronic structure in determining the dimension of NLO and TPA properties. We have demonstrated that metalloporphyrins with strong CT transition band have β values as well as TPA properties that are an order of magnitude larger than those of the porphyrin without metal. Even within the transition metal porphyrins, variation of metal ions enhances the β values about half an order magnitude and δ_{max} by at least an order of magnitude. Such amplification of chromophore polarizability through the engineering of metal-to-macrocycle charge-transfer character along the D-to-A molecular axis suggest a very good approach to enhance optical properties of porphyrin materials and new design direction for two-photon optical compounds

which can have several advantageous. We have demonstrated that the β values of dimer and trimer are about an order magnitude higher than that of monomers. Therefore, a well-designed metal D−A prophyrin (DAP) system could be an excellent candidate for application in second harmonic generation as well as for electrooptic devices based on the Pockels effect. We have shown that the TPA cross-section values of dimer and trimer are at least 2 orders magnitude higher than that of monomers. The large enhancement of two-photon absorption in dimer and trimer has potential for application in imaging, and localized activation of photochemical processes. An important consequence of the extremely high TPA cross-section is, one can use very low laser intensity to produce a given fluorescence signal, which can be of significance in biological applications. We believe that push−pull porphyrin dimer and trimers are interesting systems with potential to increase the impact of two-photon processes in photonics, materials processing, chemical sensing, and biological applications.

Acknowledgment. We thank the NSF-PREM grant DMR-0611539 for generous funding and the Mississippi Center for Super Computer Resource (MCSR), University of Mississippi, Oxford, MS, for the generous use of their computational facilities. We also thank reviewers whose valuable suggestion improved the quality of the manuscript.

References and Notes

(1) Zyss, J. *Molecular Nonlinear Optics: Materials, Physics and Devices*; Academic Press: New York, 1994.

(2) Nalwa, H. S.; Miyata, S. *Nonlinear Optics of Organic Molecules and Polymers*; CRC Press: Boca Raton, FL, 1997.

(3) Geskin, V. M.; Lambert, C.; Bredas, J.-L. *J. Am. Chem. Soc*. **2003**, *125*, 15651−15658.

(4) Kim, T.-D.; Kang, J.-W.; Luo, J.; Jang, S.-H.; Ka, J.-W.; Tucker, N.; Benedict, J. B.; Dalton, L. R.; Gray, T.; Overney, R. M.; Park, D. H.; Herman, W. N.; Jen, A. K.-Y. *J. Am. Chem. Soc*. **2007**, *129*, 488−489.

(5) Kang, H.; Evmenenko, G.; Dutta, P.; Clays, K.; Song, K.; Marks, T. J. *J. Am. Chem. Soc*. **2006**, *128*, 6194−6205.

(6) Tancrez, N.; Feuvrie, C.; Ledoux, I.; Zyss, J.; Toupet, L.; Le Bozec, H.; Maury, O. *J. Am. Chem. Soc*. **2005**, *127*, 13474−13475.

(7) Chung, S.-J.; Zheng, S.; Odani, T.; Beverina, L.; Fu, J.; Padilha, L. A.; Biesso, A.; Hales, J. M.; Zhan, X.; Schmidt, K.; Ye, A.; Zojer, E.; Barlow, S.; Hagan, D. J.; Van Stryland, E. W.; Yi, Y.; Shuai, Z.; Pagani, G. A.; Bredas, J. L.; Perry, J. W.; Marder, S. R. *J. Am. Chem. Soc*. **2006**, *128*, 14444−14445.

(8) Xu, H.-L.; Li, Z.-R.; Wu, D.; Wang, B.-Q.; Li, Y.; Gu, F. L.; Aoki, Y. *J. Am. Chem. Soc*. **2007**, *129*, 2967−2970.

(9) Avramopoulos, A.; Papadopoulos, M. G.; Reis, H. *J. Phys. Chem. B* **2007**, *111*, 2546−2553.

(10) Coe, B. J.; Jones, L. A.; Harrs, J. A.; Brunschwig, B. S.; Asselberghs, I.; Clays, K.; Persoons, A.; Garin, J.; Orduna, J. *J. Am. Chem. Soc*. **2004**, *126*, 388013.

(11) Humphrey J. L.; Kuciauskas, K. *J. Am. Chem. Soc*. **2006**, *128*, 3902.

(12) Duncan, T. V.; Susumu Sinks, L. E.; Therien, M. J. *J. Am. Chem. Soc*. **2006**, *128*, 9000.

(13) Susumu, K. Duncan, T. V.; Therien, M. J. *J. Am. Chem. Soc*. **2005**, *127*, 5186.

(14) Susumu, K.; Frail, P. R.; Angiolillo, P. J.; Therien M. J. *J. Am. Chem. Soc*. **2006**, *128*, 8380.

(15) Suslick, K. S.; Chin-Ti, C.; Meredith, G. R. *J. Am. Chem. Soc*. **1992**, *114*, 6928.

(16) Sen, A.; Ray, P. C.; Das, P. K.; Krishnan, V. *J. Phys. Chem*. **1996**, *100*, 19611.

(17) Zhang, T. G.; Zhao, Y.; Asselberghs, I.; Persoons, A.; Clays, K.; Therien, M. J. *J. Am. Chem. Soc.* **2005**, *127*, 9710.

(18) Uyeda, H.; Tetsuo, Z. Yuxia, W.; Wostyn, K.; Asselberghs, I.; Clays, K.; Persoons, A.; Therien, M. J. *J. Am. Chem. Soc*. **2002**, *124*, 13806.

(19) LeCourse, S. M.; Guan, H. W.; DiMagno, S. G.; Wang, C. H.; Therien, M. J. *J. Am. Chem. Soc.* **1996**, *118*, 1497.

(20) Ray, P. C. *Chem. Phys. Lett*. **2004**, *395*, 269.

(21) Zuhail, S.; Ray, P. C. *J Phys. Chem. A* **2005**, *109*, 9095.

(22) Bublitz, G. U.; Ortiz, R.; Runser, C.; Fort, A.; Barzoukas, M.; Marder, S. R.; Boxer, S. G. *J. Am. Chem. Soc.* **1997**, *119*, 2311.

(23) Dorr, M.; Zentel, R.; Dietrich, R.; Meerholz, K.; Brauchle, R.; Wichern, J.; Boldt, P. *Macromolecules* **1998**, *31*, 1454.

(24) Liakatas, A.; Cai, M.; Bosch, M.; Jager, C.; Bosshard, P.; Gunter, P.; Zhang, C.; Dalton, L. R. *Appl. Phys. Lett*. **2000**, *76*, 1368.

(25) Ray, P. C.; Leszczynski, J. *Chem. Phys. Lett.* **2006**, *419*, 578.

(26) Ramasesha, S.; Shuai, Z.; Bredas, J. L. *Chem. Phys. Lett.* **1995**, *245*, 226.

(27) Ray, P. C.; Ramasesha, S.; Das, P. K. *J. Chem. Phys*. **1996**, *105*, 9633.

(28) Ray, P. C. *Chem. Phys. Lett*. **2004**, *394*, 354.

(29) Ray, P. C.; Leszczynski J. *J. Phys. Chem. A* **2005**, *109*, 6689.

(30) Datta, A.; Pati, S. K. *Chem. Eur. J.* **2006**, *12*, 2780.

(31) Arnbjerg, J.; Jimenez-Banzo, A.; Paterson, M. J.; Nonell, S.; Borrell, J. I.; Christiansen, O.; Ogilby, P. R. *J. Am. Chem. Soc.* **2007**, *129*, 5188.

(32) Clay, G. O.; Schaffer, C. B.; Kleinfeld, D. *J. Chem. Phys.* **2007**, *126*, 25102.

(33) Rogers, J. E.; Slagle, J. E.; McLean, D. G.; Sutherland, R. L.; Brant, M. C.; Heinrichs, J.; Jakubiak, R.; Kannan, R.; Tan, L-S.; Fleitz, P. A. *J. Phys. Chem. A* **2007**, *111*, 1899.

(34) Kim, S.; Ohulchansky, T. Y.; Pudavar, H. E.; Pandey, R. K.; Prasad, P. N. *J. Am. Chem. Soc.* **2007**, *129*, 2669.

(35) Zhang, X-B.; Feng, Ji-K.; Ren, A-M. *J. Phys. Chem. A* **2007**, *111*, 1899.

(36) Bhaskar, A.; Ramakrishna, G.; Hagedorn, K; Varnavski, O.; Mena-Osteritz, E.; Baeuerle, P.; Goodson, T, III. *J. Phys. Chem. B* **2007**, *111*, 946.

(37) Kato, S-I.; Matsumoto, T.; Shigeiwa, M.; Gorohmaru, H.; Maeda, S. T.; Ishi-i Mataka, S. *Chem. A. Eur. J.* **2006**, *12*, 2303−2317.

(38) Kim, H. M.; Yang, W. J.; Ho Kim, C.; Park, W-H.; Jeon, S-J.; Cho, B. R. *Chem. A. Eur. J.* **2005**, *11*, 6386−6391.

(39) Das, S.; Nag, A.; Goswami, D.; Bharadwaj, P. K. *J. Am. Chem. Soc.* **2006**, *128*, 402−403.

(40) Ahn, T. K.; Kim, S. K.; Kim, D. Y.; Noh, S. B.; Aratani, N.; Ikeda, C.; Osuka, A.; Kim, D. *J. Am. Chem. Soc.* **2006**, *128*, 1700−1704.

(41) Drobizhev, M.; Stepanenko, Y.; Rebane, A.; Wilson, C. J.; Screen, T. E. O.; Anderson, H. L. *J. Am. Chem. Soc.* **2006**, *128*, 12432−12433.

(42) Woo, H. Y.; Liu, B.; Kohler, B.; Korystov, D.; Mikhailovsky, A.; Bazan, G. C. *J. Am. Chem. Soc.* **2005**, *127*, 14721−14725.

(43) Bartholomew, G. P.; Rumi, M.; Pond, S. J. K.; Perry, J. W.; Tretiak, S.; Bazan, G. C. *J. Am. Chem. Soc*. **2004**, *126*, 11529−11542.

(44) Zalesny, R.; Bartkowiak, W.; Styrcz, S.; Leszczynski, J. *J. Phys. Chem. A* **2002**, *106*, 4032.

(45) Pati, S. K.; Marks, T. J.; Ratner, M. A. *J. Am. Chem. Soc*. **2001**, *123*, 7287−7291.

(46) Chung, S. J.; Rumi, M.; Alain, V.; Barlow, S.; Perry, J. W.; Marder, S. R. *J. Am. Chem. Soc*. **2005**, *127*, 10844−10845.

(47) Collini, E.; Ferrante, C.; Bozio, R. *J. Phys. Chem. B* **2005**, *109*, 2−5.

(48) Ahn, T. K.; Kwon, J. H.; Kim, D. Y.; Cho, D. W.; Jeong, D. H.; Kim, S. K.; Suzuki, M.; Shimizu, S.; Osuka, A.; Kim, D. *J. Am. Chem. Soc.* **2005**, *127*, 12856−12861.

(49) Drobizhev, M.; Stepanenko, Y.; Dzenis, Y.; Karotki, A.; Rebane, A.; Taylor, P.; Anderson, H. L. *J. Phys. Chem. B* **2005**, *109*, 7223−7236.

(50) Kim, D. Y.; Ahn, T. K.; Kwon, J. H.; Kim, D.; Ikeue, T.; Aratani, N.; Osuka, A.; Shigeiwa, M.; Maeda, S. J. *J. Phys. Chem. A* **2005**, *109*, 2996−2999.

(51) Ogawa, K.; Ohashi, A.; Kobuke, Y.; Kamada, K.; Ohta, K. *J. Phys. Chem. B* **2005**, *109*, 22003−22012.

(52) Drobizhev, M.; Stepanenko, Y.; Dzenis, Y.; Karotki, A.; Rebane, A.; Taylor, P. N.; Anderson, H. L. *J. Phys. Chem. B* **2005**, *109*, 7223−7236.

(53) Woo, H. Y.; Korystov, D.; Mikhailovsky, A.; Nguyen, T. Q.; Bazan, G. C. *J. Am. Chem. Soc*. **2005**, *127*, 13794−13795.

(54) Zheng, Q.; He, G. S.; Prasad, P. N. *Chem. Mater.* **2005**, *17*, 6004−6011.

(55) Wang, Y.; He, G. S.; Prasad, P. N.; Goodson, T., III. *J. Am. Chem. Soc.* **2005**, *127*, 10128−10129.

(56) Zhou, X.; Ren, Ai-M.; Feng, Ji-K. *Chem. Eur. J.* **2004**, *19*, 5623−5631.

(57) Ray, P. C.; Sainudeen, Z. *J. Phys. Chem. A* **2006**, *110*, 12342−12347.

(58) Luo, Y.; Oscar, R. P.; Guo, J-D.; Agren, H. *J. Chem. Phys.* **2005**, *122*, 96101−96102.

(59) Masunov, A.; Tretiak, S. *J. Phys. Chem. B* **2004**, *108*, 899−907.

(60) Ogawa, K.; Hasegawa, H.; Inaba, Y.; Kobuke, Y.; Inouye, H.; Kanemitsu, Y.; Kohno, E.; Hirano, T.; Ogura, S.-i.; Okura, I. *J. Med. Chem.* **2006**, *49*, 2276−2283.

(61) Gao, D.; Agayan, R. R.; Xu, H.; Philbert, M. A.; Kopelman, R. *Nano Lett.* **2006**, *11*, 2383−2386.

(62) Jha, P. C.; Das, J. M.; Ramasesha, S. *J. Phys. Chem. A* **2004**, *108*, 6279−6283.

(63) Onsager, L. *J. Am. Chem. Soc*. **1936**, *58*, 1486.

(64) Tomasi, J.; Mennucci, B.; Cammi, R. *Chem. Rev.* **2005**, *105*, 2999.
(65) Frisch, M. I.; Trucks, G. W.; Schlegel, H. B.; Pople, J. A. *Gaussian 03*, revision A 11; Gaussian Inc.: Pittsburg, PA, 2003.
(66) Hay, P. J.; Wadt, W. R. *J. Chem. Phys*. **1985**, *82*, 270.
(67) Wondimagegen, T.; Ghosh, A. *J. Phys. Chem. B* **2000**, *104*, 10858.
(68) Hay, P. J. *J. Phys. Chem. A* **2002**, *106*, 1634.
(69) Setvens, W. J.; Basch, H.; Krauss, M. J. M. *J. Chem. Phys*. **1984**, *81*, 6027−6033.
(70) Dreuw, A.; Gordon, M. H. *J. Am. Chem. Soc*. **2000**, *104*, 4755,-4759.
(71) Kotzian, M.; Rosch, N.; Schroder, H.; Zerner, M. C. *J. Am. Chem. Soc*. **1989**, *111*, 7687.
(72) Zhu, L.; Yi, Y.; Shuai, Z.; Schmidt, K.; Zojer, E. *J. Phys. Chem. A* **2007**, *111*, 8509.
(73) Kanis, D. R.; Lacroix, P. G.; Ratner, M. A.; Marks, T. J. *J. Am. Chem. Soc*. **1994**, *116*, 10089.
(74) Hendrickx, E. Clays, K.; Persoons, A. *Acc. Chem. Res*. **1998**, *31*, 675.
(75) Bershon, R.; Pao, Y. H.; Frish, H. L. *J. Chem. Phys*. **1966**, *45*, 3484.
(76) Oudar, J. L. *J. Chem. Phys*. **1977**, *67*, 446.
(77) Gouterman, M. *J. Mol. Spectrosc*. **1961**, *6*, 138−163.